Chapter 2
Self-Interference-Cancellation in Full-Duplex Systems

Abstract This chapter provides a brief overview of several important concepts related to SI-cancellation techniques to form a solid background for the following chapters. We first discuss the nature of the self-interference (SI) channel which leads to the use of the analog RF cancellation stage and the digital cancellation stage. We describe both stages and state their advantages and limitations. The next part presents a quick survey on self-interference channel estimation. We then discuss the transmitter impairments that can degrade the SI-cancellation performance and the existing methods to mitigate them. The last part presents recent advances in precoding for SI-cancellation.

2.1 SI Channel Modelling

Various measurements have been done to characterise the SI channel. Consider the simple and popular architecture using the same antenna to transmit and receive via a 3-port circulator, the dominant paths of the SI channel come from the leakage through the circulator and the internal antenna reflections due to the impedance mismatch between the isolator and the antenna. On the other hand, external reflections from closely-located objects may occur with much larger delays and weaker levels compared to the dominant paths since they travel longer distances. It was reported in [1] that the external reflections are about 30 dB lower than the leakage and antenna reflections paths. When using two different antennas to transmit and receive, the line-of-sight (LoS) components and the path coming from the electromagnetic waves reflected from the transceiver structure represent the most significant paths [2, 3]. Figure 1.4 represents the different reflections that constitute the SI channel for the two antenna configurations. In both cases, the internal reflections are static since they depend on the structure of the transceiver while the external reflections vary according to the surrounding environment. In general, the power delay profile (PDP) of the SI channel is written as [1]:

$$\mathrm{PDP}(t,\tau) = \gamma_{m_1}\delta(t-\tau_{m_1}) + \gamma_{m_2}\delta(t-\tau_{m_2}) + \sum_{l=2}^{L}\gamma_l\delta(t-\tau_l), \tag{2.1}$$

T. Le-Ngoc, A. Masmoudi, *Full-Duplex Wireless Communications Systems*,
Wireless Networks, DOI 10.1007/978-3-319-57690-9_2

where $(\gamma_{m_1},\ \tau_{m_1})$ and $(\gamma_{m_2},\ \tau_{m_2})$ are the power/delay of the internal/coupling reflections and $(\gamma_l,\ \tau_l)$, for $l = 2, \ldots,\ L$ are the power/delay of the external reflections.

2.2 Analog RF Cancellation Stage

There are extensive works that describe the analog RF cancellation. Traditionally, the analog RF cancellation uses the knowledge of the transmitted SI to cancel it before the receive LNA. A copy of the transmitted signal is obtained from the PA output and passed through a cancelling circuit to reconstruct a copy of the received SI. The signal at the PA output includes the distortions of the transmitter, which are reduced by the analog RF cancellation stage.

The design of the cancelling circuit is highly related to the nature of the SI channel. As discussed in Sect. 2.1, the SI channel can be divided into internal reflections with a smaller number of paths, shorter delays and stronger amplitudes compared to the external (far-field) reflections. The internal reflections are static as they depend on the internal components and the structure of the transceiver, while the external reflections vary according to the surrounding environment. Since it is difficult to adapt the analog circuits with the variations of the external reflections, the analog RF cancellation stage reduces the static internal reflections. A cancelling circuit based on balanced transformer, such as a QHx220 chip, is used in [4, 5]. The chip takes the transmitted SI as input, changes its amplitude and its phase to match the received SI then subtracts the resulting signal from the received signal. This method achieves about 20 dB reduction in the received SI [4]. Another solution consists of using tapped delay lines (TDL) of variable delays and tunable attenuators to model the SI channel. The lines are then collected back, added up and the resulting signal is then subtracted from the received signal. Figure 2.1 shows the described TDL structure. Tuning algorithms are used to find the optimal coefficients for the attenuator, the phase shifter and the tunable delay line of each tap. The parameters of the circuit are adjusted to minimize the residual energy after cancellation [5, 6] or to minimize the error between the response of the circuit and the internal reflections response [7]. The SI reduction of the TDL varies from 30 to 45 dB [6, 7]. While the TDL can match the short delay of the internal reflections, the interaction between the delays and attenuators makes the tuning very complex. Also, analog RF cancellation is much more challenging for MIMO systems since it requires adapting different TDLs for each transmit-receive antenna pair.

As the analog RF cancellation can reduce the SI by a maximum of 45 dB, a large amount of SI is left to be reduced in the following cancellation stages. In particular, the external reflections need more adaptive cancellation methods, which can be done using digital signal processing.

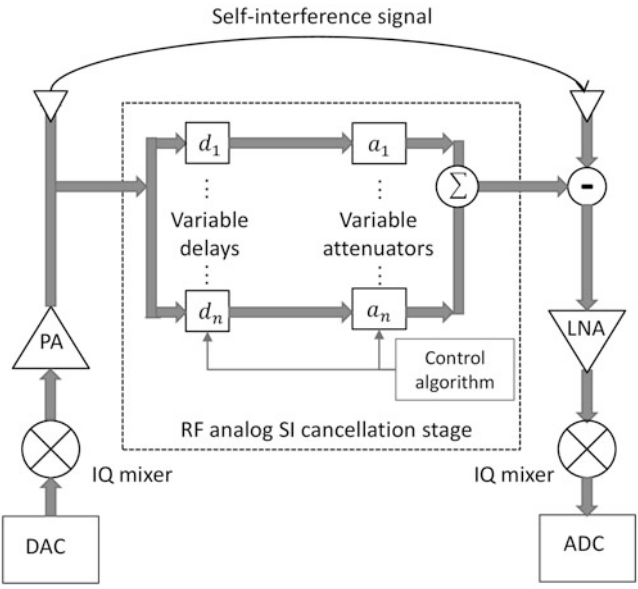

Fig. 2.1 RF analog cancellation stage

2.3 Digital SI-Cancellation

Processing the SI in the digital domain facilitates the use of adaptive digital filtering for a large number of reflected paths due to the external environment. The digital SI-cancellation is based on the general transversal symbol-synchronous finite impulse response (FIR) structure shown in Fig. 2.2, where the constant tap-delay is equal to the signal sampling period and implemented as a D-flipflop clocked by the sampling clock. Here, only the tap-coefficients need to be specified from an estimate of the SI channel and thus we avoid the interaction between the delays and the attenuations as it is the case for the analog TDL. As a result, the digital processing can deal with a larger number of taps than the analog TDL to adapt to the varying external environment. Digital SI-cancellation is particularly suitable for MIMO systems as the cross interference between antennas increases considerably the number of taps needed to reduce the SI.

The resulting cancelling signal can be subtracted from the received signal at the RF input of the LNA/ADC to further reduce the SI resulting from the external reflections and to keep the LNA/ADC not overloaded. This operation requires an additional digital-to-analog converter (DAC) and an up-converting radio chain to generate the RF signal. The additional components will slightly change the generated SI leading to residual SI. This RF cancellation stage can provide 30 dB of SI-cancellation [8, 9], which, on top of the previously-obtained 45 dB, still leaves a large amount of SI. Therefore, the baseband cancellation stage represents the last

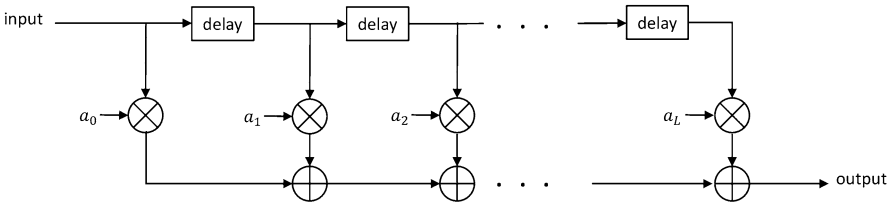

Fig. 2.2 Symbol-synchronous transversal FIR structure

line of defense against the SI by reducing it after the ADC. For this, we should estimate the transmitter nonlinearities and the residual SI channel, resulting from the difference between the actual SI channel and the equivalent channel generated by the previous cancellation stages.

2.4 Channel Estimation in Full-Duplex Systems

As previously mentioned, knowing the SI channel is an important step to reconstruct the cancelling signal. In a practical environment, it is difficult, if not impossible, to completely cancel the SI due to imperfect channel estimation [10]. In the presence of the intended signal, the received signal is expressed as:

$$y(n) = \sum_{l=0}^{L} \left(x(n-l)h^{i}(l) + s(n-l)h^{us}(l) \right) + w(n), \tag{2.2}$$

where $h^{i}(l)$ and $h^{us}(l)$ are the SI and intended channels, respectively, $(L+1)$ is the number of paths and $x(n)$ and $s(n)$ are the transmitted SI and intended signals, respectively. By collecting N observations, the resulting vector $\boldsymbol{y} = [y(1),\ y(2), \ldots,\ y(N)]^{T}$ is expressed as:

$$\boldsymbol{y} = \boldsymbol{X}\boldsymbol{h}^{i} + \boldsymbol{S}\boldsymbol{h}^{us} + \boldsymbol{w}, \tag{2.3}$$

where $\boldsymbol{X}$ and $\boldsymbol{S}$ are Toeplitz matrices obtained from the known transmitted SI signal and the unknown intended signal, respectively, $\boldsymbol{h}^{i} = \left[h^{i}(0),\ h^{i}(1), \ldots,\ h^{i}(L)\right]^{T}$ and $\boldsymbol{h}^{us} = [h^{us}(0),\ h^{us}(1), \ldots,\ h^{us}(L)]^{T}$. The existing methods follow a data-aided approach to estimate the SI channel by exploiting the knowledge of the SI data. In [8], the SI channel coefficients are obtained in the frequency domain by dividing the received signal by the known transmitted symbols over each subcarrier. A two-step Least square (LS)-based estimator is presented in [11] where a first estimate of the SI channel is obtained by considering the intended signal from the other transceiver as additive noise. After that, the interference is suppressed and the resulting signal is used to detect the intended data. A more precise estimate of the channel is

then obtained by jointly estimating the SI and intended channels using the known transmitted interference and detected data. However, an initial estimate of the signal channel is important in the detection of the intended data. Minimum mean square error (MMSE) and LS channel estimators are also used in [12] and [13] for full-duplex relays and MIMO transceivers, respectively. In general, a linear estimate of $\boldsymbol{h}^i$ is given by [14]:

$$\widehat{\boldsymbol{h}}^i = \boldsymbol{M}\boldsymbol{y}, \tag{2.4}$$

where the matrix $\boldsymbol{M}$ (to be derived) determines the estimate of $\boldsymbol{h}^i$. For example, using the LS criterion, $\boldsymbol{M}$ will be given by $(\boldsymbol{X}^H\boldsymbol{X})^{-1}\boldsymbol{X}^H$, while using the MMSE criterion:

$$\boldsymbol{M} = \left(\left(\mathbb{E}\left\{\boldsymbol{h}^i\boldsymbol{h}^{iH}\right\}\right)^{-1} + \frac{1}{\sigma^2+\sigma_s^2}\boldsymbol{X}^H\boldsymbol{X}\right)^{-1}\frac{1}{\sigma^2+\sigma_s^2}\boldsymbol{X}^H, \tag{2.5}$$

where $\mathbb{E}\{\cdot\}$ denotes statistical expectation and σ^2 and σ_s^2 are the variances of the thermal noise and the intended signal, respectively. While the latter needs the knowledge of the second-order statistics of the SI channel, it enjoys substantially lower channel estimation error than the LS estimator.

An adaptive least mean square (LMS) algorithm to estimate the SI channel is also proposed in [15] and [16] where the large SI signal compared to the intended signal is exploited to obtain an estimate of the SI channel. However, many iterations are needed for the algorithm to converge during which it is not possible to recover the intended signal. A power allocation strategy is presented in [17] to improve the estimate of the SI channel. This strategy leads to a higher power employed to estimate the channel and less power is left for data transmission, which has the advantage of obtaining an accurate SI channel estimate but low data transmission rate.

The above-mentioned methods were motivated by the knowledge of the transmitted SI, leading to simple estimators. However, they only estimate the SI channel, making the intended signal behaves as additive noise. This increases the overall noise during the estimation process and will ultimately degrade the performance of these methods which limits the cancellation capability of full-duplex systems. Given the high requirement of the estimation accuracy, it is important to find more efficient algorithms that can estimate the desired SI channel without being affected by the intended signal. One direct solution is to set a training period during which only the transceiver itself is transmitting, and thus receiving only the SI to properly estimate the SI channel. The downside of this solution is the decrease in the throughput as the two communicating transceivers need to reserve one period each in a periodic manner to update the estimated coefficients when the SI-channel changes. Another approach is to incorporate the intended signal in the estimation process by jointly estimating the SI and intended channels. As the intended signal is unknown, the intended channel can be estimated blindly or semi-blindly if some pilot symbols are transmitted from the intended transceiver. Moreover, in most of

the above-mentioned methods, the impairments of the RF components have not been considered and their effects cannot be cancelled which leaves a large amount of SI. As will be discussed in Chap. 3, reducing the transmitter impairments is primordial to properly detect the intended signal, and thus they have to be estimated and cancelled.

Spatial domain cancellation attempts to reduce the SI by precoding at the transmit chain and decoding at the receive chain [18, 19]. As detailed in Sect. 2.7, these techniques require the knowledge of both the SI and intended channels which motivates more the development of channel estimators for full-duplex systems.

2.5 Effect of Transmitter Impairments in SI-Cancellation

In order to subtract the received SI, we need to capture every modification that can occur to the transmitted SI. This includes the propagation channel and the responses of the transceiver components such as the IQ mixer and the PA. Actually, the transmitted SI is slightly modified as it goes through the transmit chain. While these modifications are relatively low compared to the main signal, they are of significant magnitude compared to the intended signal and thus will limit the performance of the full-duplex system. In most practical implementations, the inband image resulting from the transmit IQ mixer is about 30 dB lower than the direct signal [20]. In the presence of strong SI of about 50 dB higher than the intended signal, this IQ image represents additional interference for the intended signal and has to be also reduced. Several recent studies have been performed to analyze a selection of the transceiver component's impairments in the particular context of full-duplex [21–26]. We mention here that alternative high-speed DAC provides a direct conversion of the baseband signal to the RF frequency, resulting in an architecture known as a direct RF transmitter. This approach can avoid many distortions related to the up-conversion. Until now, the high-speed DACs have been only used for low frequency transmission or military communications.

In [23, 25], it was observed that the phase noise generated by the local oscillators can potentially limit the SI-cancellation capability when independent oscillators are used in the up-conversion and down-conversion. A shared-oscillator can reduce the phase noise effects and improve the cancellation performance by 25 dB [26]. In this case, the difference between the phase noise affecting the transmitted and received SI depends on the propagation delay that the SI experiences from the transmit to receive chains. A comprehensive analysis of the transceiver impairments that does not include the phase noise effects is provided in [21] and showed that nonlinear cancellation techniques should be implemented to properly reduce the SI. Such techniques can reduce the effects of the PA in the baseband cancellation stage by estimating the nonlinear coefficients of the PA [27] and another technique has been proposed to deal with the IQ mixer imbalance in [28].

2.6 Cancellation of Nonlinear Distortions

Transmitter imperfections, including the PA nonlinearity and the IQ imbalance, are significant limiting factors that bound the SI cancellation capability. To reduce these impairments, their effects should be properly modeled. The response of the PA is usually approximated by a Hammerstein model as [29, 30]:

$$x^{PA}(t) = \left(\sum_{p=0}^{P} \alpha_{2p+1} x(t) |x(t)|^{2p} \right) \star f(t), \tag{2.6}$$

where α_{2p+1}, for $p = 0, \ldots, P$, are the complex-valued polynomial coefficient for a nonlinearity order of P, and $f(t)$ is the memory of the PA. In (2.6), $\star$ denotes the convolution operator.

An iterative technique is proposed in [27] to jointly estimate the SI channel and the nonlinearity coefficients required to suppress the distorted signal. The analysis in [27] is limited to memoryless PA (i.e., $f(t) = \delta(t)$) and to the third-order nonlinearity (considers only α_3) simplifying (2.6) into:

$$x^{PA}(t) = x(t) + \alpha_3 x(t) |x(t)|^2. \tag{2.7}$$

Considering a multipath propagation channel, the received signal at the ADC output is written as:

$$y(n) = \sum_{l=0}^{L} \left(h^{i}(l) x(n-l) + h^{us}(l) s(n-l) \right) + d(n) + w(n), \tag{2.8}$$

where $d(n)$ collects the PA nonlinearity and the SI channel and $w(n)$ is the additive Gaussian noise. In [27], an iterative estimation technique is proposed by following these steps:

1. An initial estimate of the SI channel is obtained using the LS criterion and considering $\sum_{l=0}^{L} h^{us}(l) s(n-l) + d(n)$ as additive noise.
2. The previous estimated channel is used to find the nonlinear coefficients.
3. $d(n)$ is reconstructed and subtracted from the received signal to estimate again the SI channel.

The SI image resulting from the IQ imbalance can be attenuated by using a widely-linear representation of the received signal [22]. Actually, the output of an IQ mixer is:

$$x^{IQ}(t) = g_1 x(t) + g_2 x^{*}(t), \tag{2.9}$$

where g_1 and g_2 represent the response to the direct signal and the image signal, respectively. Using (2.9) to model the transmitter and the receiver IQ mixers, the discrete-time received signal is given by:

$$\begin{aligned} y(n) &= \sum_{l=0}^{L} h^i(l) x^{IQ}(n-l) + r(n) \\ &= \sum_{l=0}^{L} h_1^i(l) x(n-l) + h_2^i(l) x^*(n-l) + r(n), \end{aligned} \tag{2.10}$$

where $r(n)$ denotes the sum of all other signal, including the intended signal from the other transceiver, the thermal noise and the PA-induced nonlinearity; $h_1^i(l)$ is the equivalent SI channel of the transmitted signal $x(n)$; and $h_2^i(l)$ is the equivalent channel of the image signal $x^*(n)$ resulting from the IQ imbalance. The authors of [28] observed that the IQ imbalance can be mitigated if an estimate of $h_2^i(l)$ is available. Therefore, they estimate both $h_1^i(l)$ and $h_2^i(l)$ from the observed signal $y(n)$ based on the known transmitted signal $x(n)$ and its complex conjugate $x^*(n)$. Gathering N observations, the resulting vector $\boldsymbol{y} = [y(1), \ldots, y(N)]^T$ is expressed as:

$$\begin{aligned} \boldsymbol{y} &= \boldsymbol{X}\boldsymbol{h}_1^i + \boldsymbol{X}^*\boldsymbol{h}_2^i + \boldsymbol{r} \\ &= \underbrace{[\boldsymbol{X}\ \boldsymbol{X}^*]}_{\boldsymbol{X}_{aug}} \underbrace{\begin{pmatrix} \boldsymbol{h}_1^i \\ \boldsymbol{h}_2^i \end{pmatrix}}_{\boldsymbol{h}_{aug}} + \boldsymbol{r}, \end{aligned} \tag{2.11}$$

where $\boldsymbol{X}$ is a Toeplitz matrix obtained from the known transmitted SI signal, $\boldsymbol{X}^*$ is its complex conjugate, $\boldsymbol{h}_1^i = \left[h_1^i(0),\ h_1^i(1), \ldots,\ h_1^i(L)\right]^T$ and $\boldsymbol{h}_2^i = \left[h_2^i(0),\ h_2^i(1), \ldots,\ h_2^i(L)\right]^T$. Using these notations, the LS estimator of $\boldsymbol{h}_{aug}$ is obtained as:

$$\widehat{\boldsymbol{h}}_{aug} = (\boldsymbol{X}_{aug}^H \boldsymbol{X}_{aug})^{-1} \boldsymbol{X}_{aug}^H \boldsymbol{y}, \tag{2.12}$$

where the use of the reference signal and its complex conjugate is referred to as widely-linear estimation.

A more general approach presented in [31] takes into account the effects of both PA nonlinearities and IQ imbalance. The proposed estimator in [31] is similar to the one in [28] and the estimated vector containing the SI channel and the nonlinear parameters is given by:

$$\widehat{\boldsymbol{h}} = [\boldsymbol{X}_{\text{PA}}\ \boldsymbol{X}_{\text{PA}}^*]^{\#} \boldsymbol{y}, \tag{2.13}$$

where $\boldsymbol{X}_{\text{PA}}$ is a concatenation of P Toeplitz matrices with elements $x(n)|x(n)|^{2p}$, for $p = 0, \ldots, P$, where P is the polynomial order of the PA and the operator $(\cdot)^{\#}$ denotes the pseudo-inverse of a given matrix.

The aforementioned approaches to estimate the transmitter nonlinearities rely on linear estimators. Here too the intended signal has been ignored or treated as additive noise. As such, it should be expected that including the intended signal in the estimation process should provide significant performance increases. This could be related to blind channel estimation when the intended signal is unknown or semi-blind estimation when using the pilot symbols in conjunction with the unknown symbols.

Despite the extensive study on blind and semi-blind approaches in half-duplex transmission, very little effort has been made to apply them to parameter estimation in full-duplex systems. Due to the differences in the received signal structure, the blind and semi-blind algorithms developed for half-duplex transmission cannot be applied in full-duplex due to the following reasons. Actually, the presence of the SI and intended signal makes the number of parameters to estimate larger than in half-duplex. Also, we need to reduce the transmitter impairments, which imposes a different estimation strategy. Hence, there is a need to develop new estimation algorithms that are well-adapted to the full-duplex system model. This will be treated in the following chapters.

2.7 Spatial Cancellation

Spatial cancellation, based on transmit beamforming, can be combined with the previous cancellation approaches to further reduce the SI. The signal model in this section is built upon frequency-flat channels resulting from OFDM transmission over a multipath channel. We consider that the full-duplex transceiver is equipped with N_t transmit and N_r receive antennas. The received signal can be modeled as:

$$\boldsymbol{y} = \boldsymbol{H}^{i}\boldsymbol{x} + \boldsymbol{H}^{us}\boldsymbol{s} + \boldsymbol{w}, \tag{2.14}$$

where $\boldsymbol{x} = [x_1, \ldots, x_{N_t}]^T$ and $\boldsymbol{s} = [s_1, \ldots, s_{N_t}]^T$ are the transmitted SI and intended signal from all antennas, respectively, $\boldsymbol{H}^{i}$ and $\boldsymbol{H}^{us}$ are $N_r \times N_t$ matrices representing the respective MIMO channel from the transmit stream to the receive steam of the same transceiver and between the two transceivers, and $\boldsymbol{w}$ is the $N_r \times 1$ vector collecting the thermal noise. To exploit the DoF provided by the spatial domain, the transceiver applies a $N_t \times \widetilde{N}_t$ transmit precoding matrix $\boldsymbol{G}_{Tx}$ and a $\widetilde{N}_r \times N_r$ receive decoding matrix $\boldsymbol{G}_{Rx}$ with $\widetilde{N}_t \leq N_t$ and $\widetilde{N}_r \leq N_r$ being the number of input and output dimensions (or the number of independent streams), respectively. The target is to make the received SI close to zero. Thus, the transmit signal can be

pre-processed using $\boldsymbol{G}_{Tx}$ as $\boldsymbol{x} = \boldsymbol{G}_{Tx}\widetilde{\boldsymbol{x}}$ and the received signal can be post-processed using $\boldsymbol{G}_{Rx}$ to obtain:

$$\begin{aligned}\widetilde{\boldsymbol{y}} &= \boldsymbol{G}_{Rx}\boldsymbol{y} \\ &= \boldsymbol{G}_{Rx}\boldsymbol{H}^{i}\boldsymbol{G}_{Tx}\widetilde{\boldsymbol{x}} + \boldsymbol{G}_{Rx}\boldsymbol{H}^{us}\boldsymbol{s} + \boldsymbol{G}_{Rx}\boldsymbol{w}.\end{aligned} \tag{2.15}$$

Roughly speaking, the processing matrices $\boldsymbol{G}_{Tx}$ and $\boldsymbol{G}_{Rx}$ modify the true SI channel seen by the receiver. Here, these two matrices are designed to reduce the SI given by $\boldsymbol{G}_{Rx}\boldsymbol{H}^{i}\boldsymbol{G}_{Tx}\widetilde{\boldsymbol{x}}$. One technique, called antenna selection[1] (AS) [19], selects the transmit and receive antenna pairs which lead to a minimal received SI. To that end, the transmit and receive filters are implemented to minimize[2]:

$$||\boldsymbol{G}_{Rx}\boldsymbol{H}^{i}\boldsymbol{G}_{Tx}||_{F}^{2}, \tag{2.16}$$

with[3] the additional constraint that $\boldsymbol{G}_{Rx}^{T}$ and $\boldsymbol{G}_{Tx}$ are two subset selection matrices (i.e., matrices with binary elements such that $\sum_{i}\boldsymbol{G}_{Tx}(i,j) = 1$ for all j and $\sum_{j}\boldsymbol{G}_{Tx}(i,j) \in \{0,1\}$ for all i). The filters that minimize (2.16) are obtained by calculating the Frobenius norm for all possible combinations and choosing the lowest.

The beam selection (BS) technique is based on the singular value decomposition (SVD) of the matrix $\boldsymbol{H}^{i}$ to find the transmit and receive filters [19, 32]. More specifically, by writing $\boldsymbol{H}^{i} = \boldsymbol{U}\boldsymbol{\Sigma}\boldsymbol{V}^{H}$, where $\boldsymbol{U}$ and $\boldsymbol{V}$ are unitary matrices and the diagonal matrix $\boldsymbol{\Sigma}$ comprises the singular values of $\boldsymbol{H}^{i}$, the BS is performed by first finding the subset selection matrices $\boldsymbol{S}_{Rx}$ and $\boldsymbol{S}_{Tx}$ that minimize:

$$||\boldsymbol{S}_{Rx}^{T}\boldsymbol{\Sigma}\boldsymbol{S}_{Tx}||_{F}^{2}. \tag{2.17}$$

Then, the BS matrices are chosen as:

$$\boldsymbol{G}_{Tx} = \boldsymbol{V}\boldsymbol{S}_{Tx} \text{ and } \boldsymbol{G}_{Rx} = \boldsymbol{S}_{Rx}^{T}\boldsymbol{U}^{H}. \tag{2.18}$$

The row and column selection in the BS is based on the diagonal matrix $\boldsymbol{\Sigma}$ such that the subset selection matrices $\boldsymbol{S}_{Rx}$ and $\boldsymbol{S}_{Tx}$ are chosen to select the off-diagonal elements of $\boldsymbol{\Sigma}$.

The null-space projection (NSP) has been proposed to completely eliminate the SI [19, 33–35]. In this method, $\boldsymbol{G}_{Tx}$ and $\boldsymbol{G}_{Rx}$ are selected such that the transmission and reception are performed in different subspaces, i.e., the transmit signal is

[1] This method was originally proposed for full-duplex relay station.

[2] In practical implementation, only an estimate of the SI channel is available and used in the minimization process.

[3] In (2.16), $||.||_{F}$ returns the Frobenius norm of a matrix.

projected into the null-space of the SI channel. Therefore, the filter design is stated as:

$$\boldsymbol{G}_{Rx}\boldsymbol{H}^{i}\boldsymbol{G}_{Tx} = \boldsymbol{0}. \tag{2.19}$$

The way to solve the NSP depends on the rank of the SI channel. If $\min\{N_t, N_r\}$ is larger than the rank of $\boldsymbol{H}^{i}$, the BS previously discussed provides $\boldsymbol{S}_{Rx}^{T}\boldsymbol{\Sigma}\boldsymbol{S}_{Tx} = \boldsymbol{0}$ by selecting the singular value *zero* when choosing $\boldsymbol{S}_{Rx}$ and $\boldsymbol{S}_{Tx}$. For general low rank SI channel, $\boldsymbol{G}_{Tx}$ can be chosen to belong to the right null space of $\boldsymbol{H}^{i}$ (by taking the columns of $\boldsymbol{V}$ associated with the singular value zero of $\boldsymbol{H}^{i}$) or similarly we choose $\boldsymbol{G}_{Rx}$ to belong to the left null space of $\boldsymbol{H}^{i}$. Other designs can also be adopted in the particular case of $N_t = N_r = 2$ and $\widetilde{N}_t = \widetilde{N}_r = 1$ [35].

In general, spatial cancellation requires the number of transmitting antennas to be larger than the number of receive antennas and reduces the available data stream for SI-cancellation.

2.8 Chapter Summary

This chapter provided an overview of the existing works on SI-cancellation in full-duplex wireless systems. The cancellation techniques can go from subtraction of the received SI into precoding to reduce the coupling signal. It was seen that the estimation of the SI channel is a central issue to develop efficient cancellation methods. This review provided some motivation for the material proposed in this book. In particular, we focus on the digital SI-cancellation by developing efficient estimators while the design of the RF analog cancellation is beyond the scope of the book. A CS-based estimator is presented for the RF cancellation stage, which exploits the sparsity of the SI channel. Then, subspace-based and ML algorithms are developed to estimate the residual SI and the transmitter nonlinearities for the baseband cancellation stage, in the presence of the unknown intended signal. Also, a new ASI method is proposed to substitute or complete the RF cancellation stage. Before that, a detailed study of the received SI is presented in the next chapter to help understanding its nature and developing the appropriate cancellation techniques.

References

1. X. Wu, Y. Shen, and Y. Tang, "The power delay profile of the single-antenna full-duplex self-interference channel in indoor environments at 2.6 GHz," *IEEE Antennas and Wireless Propagation Letters*, vol. 13, pp. 1561–1564, 2014.
2. C. R. Anderson, S. Krishnamoorthy, C. G. Ranson, T. J. Lemon, W. G. Newhall, T. Kummetz, and J. H. Reed, "Antenna isolation, wideband multipath propagation measurements, and interference mitigation for on-frequency repeaters," in *Proc. IEEE SoutheastCon*, Greensboro, North Carolina, USA, Mar. 2004.

3. A. Sethi, V. Tapio, and M. Juntti, "Self-interference channel for full duplex transceivers," in *Proc. IEEE Wireless Commun. and Netw. Conf.*, Istanbul, Turkey, Apr. 2014.
4. J. I. Choi, M. Jain, K. Srinivasan, P. Levis, and S. Katti, "Achieving single channel, full duplex wireless communication," in *Proc. ACM MobiCom*, Chicago, Illinois, USA, Sept. 2010.
5. M. Jain, J. I. Choi, T. Kim, D. Bharadia, S. Seth, K. Srinivasan, P. Levis, S. Katti, and P. Sinha, "Practical, real-time, full duplex wireless," in *Proc. of ACM Mobicom*, Las Vegas, Nevada, USA, Sept. 2011.
6. D. Bharadia, E. McMilin, and S. Katti, "Full duplex radios," in *Proc. of the ACM SIGCOMM 2013*, Hong Kong, China, Aug. 2013.
7. K. E. Kolodziej, J. G. McMichael, and B. Perry, "Adaptive RF canceller for transmit-receive isolation improvement," in *IEEE Radio and Wireless Symposium (RWS)*, Newport Beach, California, USA, Jan. 2014.
8. M. Duarte, C. Dick, and A. Sabharwal, "Experiment-driven characterization of full-duplex wireless systems," *IEEE Trans. Wireless Comm.*, vol. 11, no. 12, pp. 4296–4307, 2012.
9. M. Duarte, A. Sabharwal, V. Aggarwal, R. Jana, K. Ramakrishnan, C. W. Rice, and N. Shankaranarayanan, "Design and characterization of a full-duplex multiantenna system for WiFi networks," *IEEE Trans. Vehicular Technology*, vol. 63, no. 3, pp. 1160–1177, 2014.
10. D. Kim, H. Ju, S. Park, and D. Hong, "Effects of channel estimation error on full-duplex two-way networks," *IEEE Trans. Vehicular Technology*, vol. 62, no. 9, p. 4667, 2013.
11. S. Li and R. D. Murch, "Full-duplex wireless communication using transmitter output based echo cancellation," in *Proc. IEEE Global Telecommun. Conf.*, Houston, Texas, USA, Dec. 2011.
12. J. Ma, G. Y. Li, J. Zhang, T. Kuze, and H. Iura, "A new coupling channel estimator for cross-talk cancellation at wireless relay stations," in *Proc. IEEE Global Telecommun. Conf.*, Honolulu, Hawaii, USA, Nov. 2009.
13. B. P. Day, A. R. Margetts, D. W. Bliss, and P. Schniter, "Full-duplex bidirectional MIMO: Achievable rates under limited dynamic range," *IEEE Trans. Signal Process*, vol. 60, no. 7, pp. 3702–3713, 2012.
14. S. M. Kay, *Fundamentals of statistical signal processing, Volume 1: Estimation theory*. Prentice Hall, 1993.
15. J. R. Krier and I. F. Akyildiz, "Active self-interference cancellation of passband signals using gradient descent," in *Proc. IEEE Pers. Indoor and Mobile Radio Commun.*, London, UK, Sept. 2013.
16. N. Li, W. Zhu, and H. Han, "Digital interference cancellation in single channel, full duplex wireless communication," in *Prog. Wireless Communications, Networking and Mobile Computing (WiCOM)*, Shanghai, China, Sept. 2012.
17. Z. Zhan, G. Villemaud, J.-M. Gorce *et al.*, "Analysis and reduction of the impact of thermal noise on the full-duplex ofdm radio," in *IEEE Radio Wireless Symposium*, Newport Beach, California, USA, Jan. 2014.
18. D. Bliss, P. Parker, and A. Margetts, "Simultaneous transmission and reception for improved wireless network performance," in *IEEE/SP Workshop on Statistical Signal Processing*, Madison, Wisconsin, USA, Aug. 2007.
19. T. Riihonen, S. Werner, and R. Wichman, "Mitigation of loopback self-interference in full-duplex MIMO relays," *IEEE Trans. Signal Process.*, vol. 59, no. 12, pp. 5983–5993, 2011.
20. "LTE; evolved universal terrestrial radio access (E-UTRA); user equipment (UE) radio transmission and reception (3GPP TS 36.101 version 11.2.0 release 11)." ETSI, Sophia Antipolis Cedex, France.
21. D. Korpi, T. Riihonen, V. Syrjala, L. Anttila, M. Valkama, and R. Wichman, "Full-duplex transceiver system calculations: Analysis of ADC and linearity challenges," *IEEE Trans. Wireless Comm.*, vol. 13, no. 7, pp. 3821–3836, 2014.
22. A. Masmoudi and T. Le-Ngoc, "Self-interference cancellation limits in full-duplex communication systems," in *Proc. IEEE Global Telecommun. Conf.*, Washington DC, USA, Dec. 2016.

23. A. Sahai, G. Patel, C. Dick, and A. Sabharwal, "On the impact of phase noise on active cancelation in wireless full-duplex," *IEEE Trans. on Vehicular Technology*, vol. 62, no. 9, pp. 4494–4510, Nov 2013.
24. A. Masmoudi and T. Le-Ngoc, "Residual self-interference after cancellation in full-duplex systems," in *Proc. IEEE Int. Conf. Commun.*, Sydney, Australia, June 2014.
25. E. Ahmed and A. M. Eltawil, "On phase noise suppression in full-duplex systems," *IEEE Trans. on Wireless Comm.*, vol. 14, no. 3, pp. 1237–1251, 2015.
26. V. Syrjala, M. Valkama, L. Anttila, T. Riihonen, and D. Korpi, "Analysis of oscillator phase-noise effects on self-interference cancellation in full-duplex OFDM radio transceivers," *IEEE Trans. on Wireless Comm.*, vol. 13, no. 6, pp. 2977–2990, June 2014.
27. E. Ahmed, A. M. Eltawil, and A. Sabharwal, "Self-interference cancellation with nonlinear distortion suppression for full-duplex systems," in *Proc. ASILOMAR Signals, Syst., Comput.*, Pacific Frove, California, USA, Nov. 2013.
28. D. Korpi, L. Anttila, V. Syrjala, and M. Valkama, "Widely linear digital self-interference cancellation in direct-conversion full-duplex transceiver," *IEEE Journal on Selected Areas in Communications*, vol. 32, no. 9, pp. 1674–1687, Sept 2014.
29. A. Masmoudi and T. Le-Ngoc, "Channel estimation and self-interference cancellation in full-duplex communication systems," *IEEE Trans. Vehicular Technology*, vol. 66, no. 1, pp. 321–334, Jan. 2017.
30. ——, "A digital subspace-based self-interference cancellation in full-duplex MIMO transceivers," in *Proc. IEEE Int. Conf. Commun.*, London, UK, June 2015.
31. L. Anttila, D. Korpi, E. Antonio-Rodríguez, R. Wichman, and M. Valkama, "Modeling and efficient cancellation of nonlinear self-interference in MIMO full-duplex transceivers," in *IEEE Globecom Workshops*, Austin, Texas, USA, Dec. 2014.
32. P. Larsson and M. Prytz, "MIMO on-frequency repeater with self-interference cancellation and mitigation." in *Proc. of IEEE VTC-Spring*, Yokohama, Japan, May 2009.
33. B. Chun and Y. H. Lee, "A spatial self-interference nullification method for full duplex amplify-and-forward MIMO relays," in *Proc. IEEE Wireless Commun. and Netw. Conf.*, Sydney, Australia, Apr. 2010.
34. B. Chun and H. Park, "A spatial-domain joint-nulling method of self-interference in full-duplex relays," *IEEE Comm. Lett.*, vol. 16, no. 4, pp. 436–438, 2012.
35. H. Ju, E. Oh, and D. Hong, "Improving efficiency of resource usage in two-hop full duplex relay systems based on resource sharing and interference cancellation," *IEEE Trans. Wireless Comm.*, vol. 8, no. 8, pp. 3933–3938, 2009.

http://www.springer.com/978-3-319-57689-3

Full-Duplex Wireless Communications Systems
Self-Interference Cancellation
Le-Ngoc, T.; Masmoudi, A.
2017, XII, 164 p. 59 illus., 51 illus. in color., Hardcover
ISBN: 978-3-319-57689-3